Journal of Achievements in Materials and Manufacturing Engineering
International Scientific Journal published monthly by the World Academy of Materials and Manufacturing Engineering

Finite elements analysis of the side grooved I-beam specimen for mode II fatigue crack growth rates determination

T.M. Lenkovskiy [a], V.V. Kulyk [b,*], Z.A. Duriagina [b,c], L.V. Dzyubyk [b], V.V. Vira [b], A.R. Dzyubyk [b], T.L. Tepla [b]

[a] Karpenko Physico-Mechanical Institute of the National Academy of Sciences of Ukraine, 5 Naukova St., Lviv 79060, Ukraine

[b] Lviv Polytechnic National University, 12 Bandera St., Lviv, 79013, Ukraine

[c] The John Paul II Catholic University of Lublin, Al. Racławickie 14, 20-950 Lublin, Poland

* Corresponding e-mail address: kulykvolodymyrvolodymyrovych@gmail.com

ABSTRACT

Purpose: Carefully investigate the stress-strain state of the side grooved I-beam specimen with edge crack and determine the effect of crack length and crack faces friction on stress intensity factor at transverse shear.

Design/methodology/approach: The finite element method was used to estimate the stress-strain state of I-beam specimen at transverse shear. For this purpose, a full-scale, three-dimensional model of the specimen was created, which precisely reproduces its geometry and fatigue crack faces contact. For the correct reproduction of the stress singularity at the crack tip, a special sub-model was used, which has been tested earlier in solving similar problems of fracture mechanics. In order to improve the accuracy of the calculations, for crack plane and cross-section of the specimen on the crack extension modeling, an algorithm for changing the crack length without changing the total number of elements in the model was developed and applied. Young's modulus and Poisson's ratio of structural steels were specified for the model material. The static loading of the model was realized assuming small scale yielding condition. The stress intensity factor was found through the displacement of nodes in the prismatic elements adjacent to the plane and the front of the crack.

Findings: Mathematical dependences, which show an increase of stress intensity factor in the I-beam specimen with an increase in the crack length, and its decrease with an increase of crack faces friction factor at transverse shear, were established. The results are compared with the partial cases known from the literature and their good convergence was shown.

Research limitations/implications: By analyzing the obtained graphical dependences, it is established that for relative crack lengths less than 0.4 there is a significant influence of the initial notch on the stress-strain state of the specimen, and for the lengths greater than 0.9 an influence of constrained gripping part took place. For this reason, all subsequent calculations were carried out in the range of relative crack length from 0.4 to 0.9, which represents the applicability range of the final calculation formula. Increasing of the crack faces friction factor from 0 to 1 monotonically reduces the stress at the crack tip. For a short crack, this effect is 1.5 times greater than for a long one, which is reflected by the calculation formula.

Practical implications: Using the proposed calculation formula, one can calculate the stress intensity factor in the I-beam specimen, and to determine the crack growth resistance characteristics of structural steels at transverse shear.

Originality/value: A new, easy-to-use in engineering calculations formula is proposed for stress intensity factor determination in the I-beam specimen at transverse shear. The formula takes into account crack faces friction for various crack lengths.

Keywords: Finite element method, Mode II fracture, Transverse shear, Stress intensity factor, I-beam specimen

Reference to this paper should be given in the following way:

T.M. Lenkovskiy, V.V. Kulyk, Z.A. Duriagina, L.V. Dzyubyk, V.V. Vira, A.R. Dzyubyk, T.L. Tepla, Finite elements analysis of the side grooved I-beam specimen for mode II fatigue crack growth rates determination, Journal of Achievements in Materials and Manufacturing Engineering 86/2 (2018) 70-77.

1. Introduction

It is known [1-3] that fatigue failure of the rolling surface of railway wheels and rails in the contact zone occurs not only by normal tension mechanism but also by a transverse shear mechanism. Regarding this, in order to assess their workability and durability, it is necessary to know the fatigue crack growth resistance characteristics of the material at transverse shear. Therefore, the experimental techniques for transverse shear fatigue cracks initiation and spreading realization need to be developed. This allows fatigue crack growth rate curves building and corresponding fatigue crack growth resistance characteristics of steels determining.

From the previous theoretical and experimental studies [4-14], it is known that such curves are difficult to build at transverse shear conditions for various reasons [15], and the results obtained from them are not always well correlated with each other. This caused the need of a detailed analysis of experimental techniques in order to improve them, as well as the development of new types of specimens and loading schemes, effective for the study of fatigue crack growth kinetics at transverse shear. In works [16-18] the side grooved I-beam specimen was developed. Tests proved the effectiveness of the specimen for Mode II fracture realization and fatigue crack growth resistance characteristics of steels determining. It was achieved due to the following factors: longitudinal guiding grooves in the specimen wall reduce the area of its net cross-section, increasing tangential stresses on the initial notch line extension; at cyclic loading the compressive stresses normal to the crack plane appear, which minimizes possible normal tension fracture (Mode I); the specimen is being loaded by symmetrical sinusoidal cycle, which provides symmetry of strain distribution in the process zone; the I-beam shape of the specimen ensures its stability at console bending and prevents its distortion, eliminating out-of-plane shear fracture (Mode III).

In the previous study [17], the influence of structural steel microstructure on the crack faces friction factor in the specimen was experimentally investigated, but the stress-strain state and the effect of friction on the stress intensity factor (SIF) K_{II} were not sufficiently studied.

2. Calculation model

Since the I-beam profile with lateral grooves represents complex geometric shape, for correct determination of SIF K_{II} a full-scale, 3D model of the specimen was created. The model (Fig. 1) completely reproduces specimen geometry, including gripping part, as well as contact conditions and friction of the crack faces.

Dementions of the model are following [17]: $L_1 = 180.0$ mm; $H_1 = 32.0$; $r = 20.0$; $L = 110.2$; $W = 27.0$; $D = 6.0$; $H = 27.8$; $T = 9.6$; $b_1 = 87.8$; $b = 72.0$; $2d = 15.9$; $e = 1.4$; $t = 3.2$; $t_0 = 1.1$; $h = 25.2$ mm. Classical 3D 20-node parallelepiped, 13-node pyramidal, modified 15-node prismatic elements were used to reproduce the singularity of stresses at the crack tip, and to reproduce contact of crack faces 8-node 2D contact elements were used (Fig. 2). The total number of elements in the model was $42 \cdot 10^3$.

For fatigue crack plane and material volume in the crack tip vicinity modeling, an original sub model [19] was used, in the base of which lies a cylindrical fragment with a mathematical cut of zero thickness (Fig. 2).

The elements near the tip of mathematical cut, representing a real crack in the specimen, were modified by shifting the middle nodes to a distance of a quarter of the side length towards the crack tip, while the length of this side was 12.5 μm. The size of the classical elements was increased in the direction from the crack front to the sub-

model faces by order of the expression $c_1 = 3.52(1 - 0.242i + 0.13i^2)$, where c_1 is the side length of the regular element adjacent to the crack plane, i is the number of the layer of regular elements and acquires only integer values. The number of layers of elements of the sub-model by thickness, i.e. in z axis direction, was chosen from the ratio $N = 4c$, where c is the size of the modified element side. The correctness of the sub model has been confirmed earlier [19] on the models of standard specimens for fracture toughness tests.

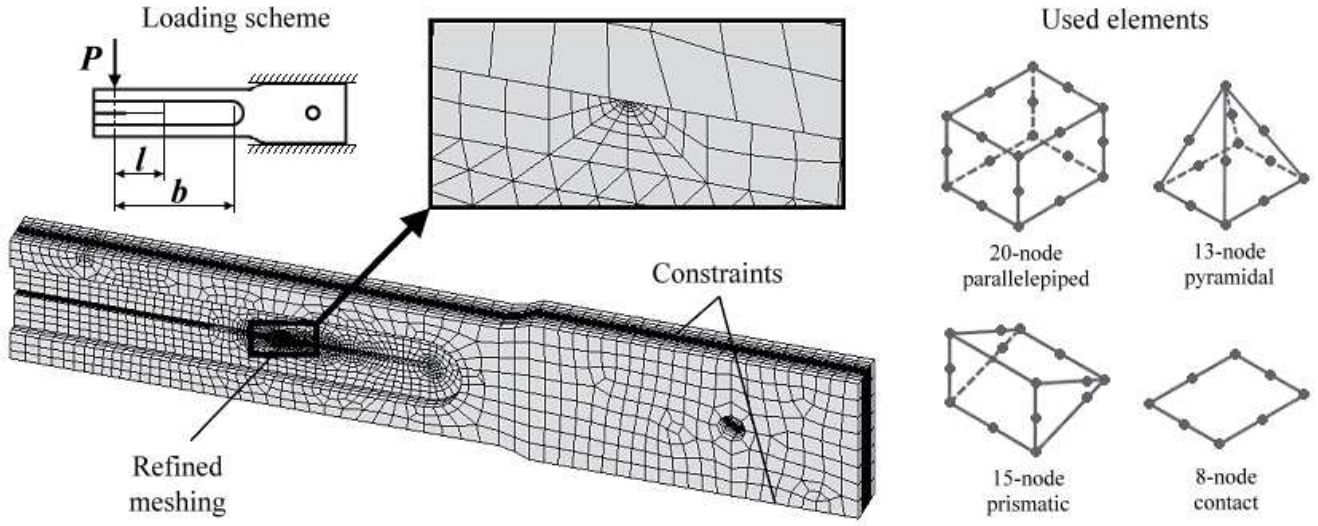

Fig. 1. Finite element model of the I-beam specimen with an edge crack

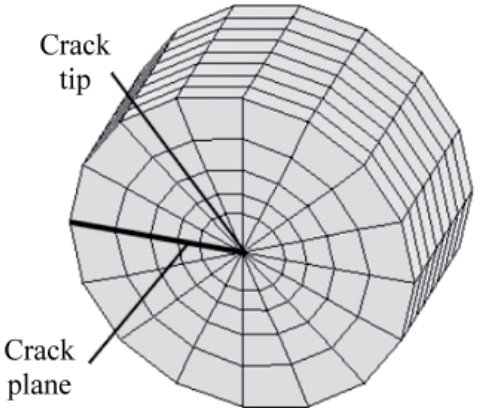

Fig. 2. Meshing of material volume near the shear crack tip

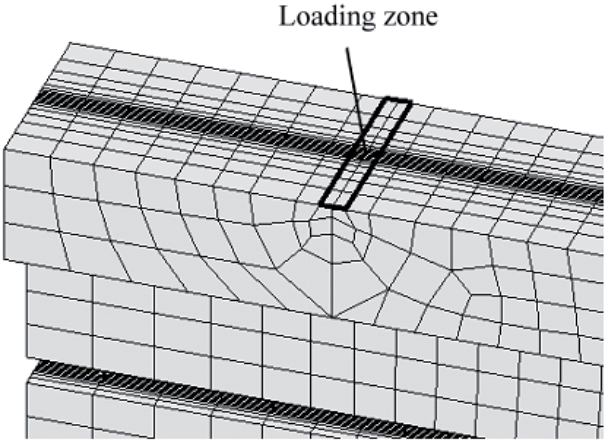

Fig. 3. Meshing the site of force applying to the model

The properties of structural steel in the model were set by Young's modulus $E = 210$ GPa and Poisson's ratio $\mu = 0.3$. The static load, assuming small scale yielding condition, was applied to the model according to the loading scheme of console bending by distributed force 1 N on the upper shelf of the free end of the model (Fig. 3). The gripping part of the model was fixed by applying appropriate constraints. It should be noted that in the vicinity of the force application site the mesh density was increased in order to achieve correct force transmission to the volume of the model.

After deforming the model by external load the displacements of nodes (no. 1…4) in the prismatic elements (side size $c = 12.5$ μm) adjacent to the crack plane and to the crack front were determined (Fig. 4).

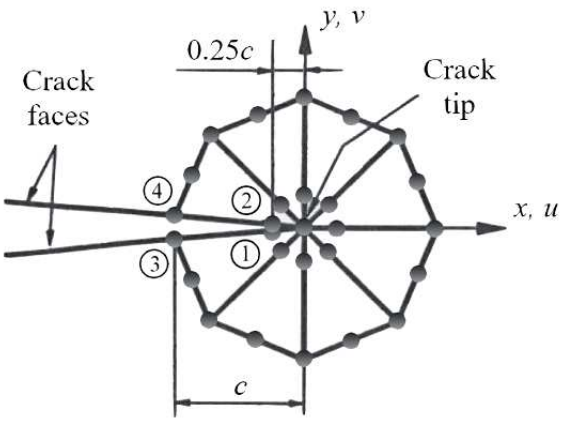

Fig. 4. Selecting the nodes for crack faces displacement determination

Since at transverse shear the crack front is bent in the direction of the initial notch (Fig. 5a), unlike normal tension, when the front is bent in the crack growth direction (Fig. 5b), it is logical to calculate SIF K_{II} through the displacements of nodes in the plane between 4th and 5th layers of prismatic elements in the crack front center. The value of these displacements will be the smallest there and will provide a larger safety factor of calculation since at the experimental determination of the crack growth resistance characteristics the fracture will occur at the lowest values of SIF K_{II}.

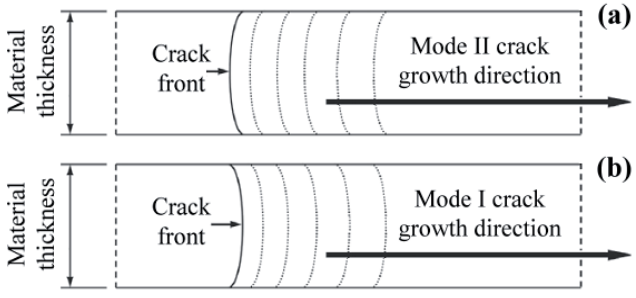

Fig. 5. Crack front shape at transverse shear (a) and at normal tension (b)

The model is adapted for SIF K_{II} determination in a wide range of crack lengths. In order to increase the accuracy of the crack plane and the cross-section of the specimen modeling, an original algorithm of changing the crack length without changing the specified number of elements in the model was developed and applied. The essence of the algorithm is that the number of elements adjoining the crack faces n_l is set by a linear function of the crack length: $n_l = f(l)$, and the number of elements on the continuation of the crack n_m by similar function $n_m = f(m)$. Since increasing of the crack length l leads to decrease of the length of the crack extension m, the increase of n_l leads to the corresponding reduction of n_m and vice versa. Meanwhile, the total number of elements of the model n_{total} remains unchanged $n_{total} = const$ (Fig. 6). For instance, if the crack length is $l = 7$, the length of solid material on its extension $m = 11$, then $n_l = 16$, $n_m = 24$, and the total number of elements $n_{total} = 120$ (Fig. 6a), then in the case when $l = 11$, $m = 7$ (Fig. 6b) the total number of elements will be $n_{total} = 120$ as well.

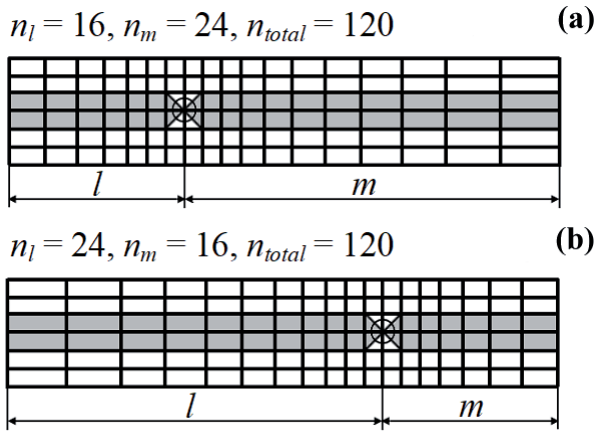

Fig. 6. Changing the crack length from short (a) to relatively long (b) without changing the total number of elements in the model

Real fatigue crack faces at transverse shear are subjected to wear, and in the unloaded specimen between the crack faces appears a gap of 0.15 mm [17]. This was taken into account when formulating the contact problem. The rigidity of crack faces when they are contacting each other under the action of external loading is determined by contact stiffness factor k_{normal}. By changing this factor we eliminate the effect of the gap, which is formed during wear of real shear crack faces.

SIF K_{II} was calculated assuming small scale yielding conditions $\kappa = 1$ for relative crack length $\lambda = l / b$ (see Fig. 1) in range from 0.36 to 0.99, using the classical formula written for transverse shear in the following form:

$$K_{II} = \frac{2G}{\chi + 1}\sqrt{\frac{\pi}{2c}}\left[\left(4u_2 - u_4\right) - \left(4u_1 - u_3\right)\right], \quad (1)$$

where $G = E / (2 (1 + \mu))$, $\chi = (3 - \mu - 4 \kappa \mu^2) / (1 + \mu)$, $u_1 \ldots u_4$ – displacements of nodes with corresponding numbers (see Fig. 4).

3. Results and their analysis

Using proposed approach to SIF K_{II} determination in the model, the graphical dependence of normalized SIF K_{II} on relative crack length λ, or *K*-calibration curve, was built (Fig. 7).

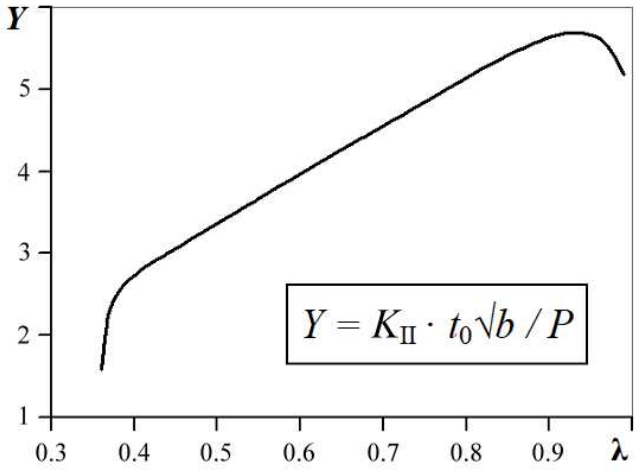

Fig. 7. Dependence of normalized SIF K_{II} on relative crack length λ in case of specimen loading by unit force P = 1 H

Analyzing this curve, it has been established that for λ < 0.4 there is the significant effect of the initial notch on the stress-strain state of the specimen, and for λ > 0,9 there is an effect of constrained gripping part. Therefore, all subsequent calculations were carried out in the range of λ from 0.4 to 0.9, where the *K*-calibration curve is almost linear. Consideration of contact interaction of crack faces gave as an opportunity to obtain graphic dependences reflecting the effect of f_c on normalized SIF K_{II} (Fig. 8). As we can see, the increase of f_c monotonically reduces normalized SIF K_{II}. For small values of λ this effect is 1.5 times greater than for large ones.

Using the least squares method, the resulting data array was approximated by a function of two variables $Y = f(\lambda, f_c)$ with maximum deviation of 4%. On this basis the formula for SIF K_{II} calculation in the range of $0.4 \le \lambda \le 0.9$ and $0 \le f_c \le 1$ is written:

$$K_{II} = \frac{P}{t_0\sqrt{H}} Y(\lambda, f_c), \tag{2}$$

where $Y(\lambda, f_c) = 0.22 + 6.29 - f_c\,(1.2\lambda + 1.34)$.

To verify correctness of the calculations, the obtained results were compared with those obtained earlier on the initial stages of the specimen development [16]. This comparison is given in Table 1.

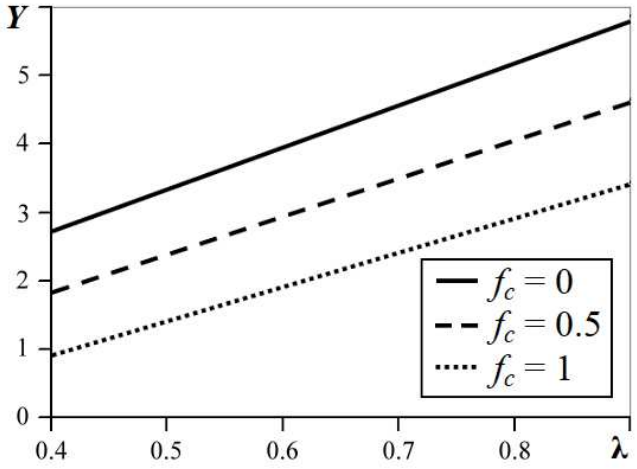

Fig. 8. Effect of crack faces friction factor f_c on normalized SIF K_{II}

The results of SIF K_{II} calculations were compared with the ones obtained by other methods. The comparison of the *K*-calibration curve with the solution obtained by the method of superposition of stressed states in [20] shows good convergence in the range of λ from 0.4 to 0.7 (Fig. 9) where maximum deviation does not exceed 5%.

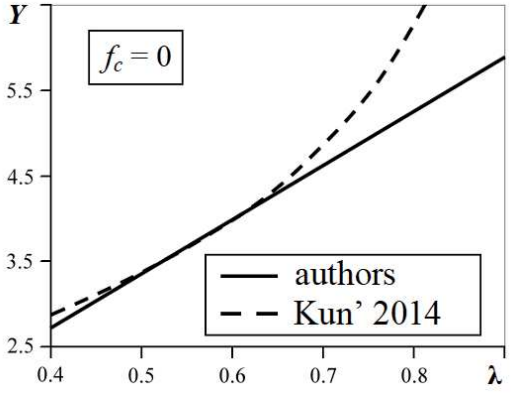

Fig. 9. Comparison of the normalized SIF K_{II} obtained by different methods

The dependence reflecting the influence of f_c on the normalized SIF K_{II} was compared with one obtained for compression of a disk specimen with an inclined central crack of relative length λ = 0.5 by the finite difference method in work [21]. As can be seen (Fig. 10), the two dependencies have a decreasing linear shape, which does not contradict with the Amonton-Coulomb model of friction stating that friction force depends only on clamping force and friction factor of surfaces.

Table 1.
Normalized SIF K_{II} for I-beam specimen with an edge crack

λ	f_c	Y_{FEM}	Y	$Y_{[16]}$	$(Y - Y_{FEM}) / Y_{FEM}$	$(Y - Y_{[16]}) / Y_{[16]}$
0.4	0.00	2.733	2.736	2.683	0.001	0.020
	0.25	2.228	2.281	2.243	0.024	0.017
	0.50	1.769	1.823	1.800	0.031	0.013
	0.75	1.396	1.371	1.355	-0.018	0.012
	1.00	0.941	0.916	–	-0.027	–
0.5	0.00	3.372	3.365	3.384	-0.002	-0.006
	0.25	2.926	2.88	2.888	-0.016	-0.003
	0.50	2.330	2.395	2.388	0.028	0.003
	0.75	1.952	1.910	1.886	-0.022	0.013
	1.00	1.482	1.425	–	-0.038	–
0.6	0.00	3.966	3.994	4.037	0.007	-0.011
	0.25	3.504	3.479	3.506	-0.007	-0.008
	0.50	2.912	2.964	2.972	0.018	-0.003
	0.75	2.409	2.449	2.433	0.017	0.007
	1.00	1.994	1.934	–	-0.030	–
0.7	0.00	4.559	4.623	4.641	0.014	-0.004
	0.25	4.086	4.078	4.098	-0.002	-0.005
	0.50	3.553	3.533	3.550	-0.006	-0.005
	0.75	2.967	2.998	2.997	0.010	0.000
	1.00	2.498	2.443	–	-0.022	–
0.8	0.00	5.143	5.252	5.199	0.021	0.010
	0.25	4.663	4.677	4.664	0.003	0.003
	0.50	4.097	4.102	4.124	0.001	-0.005
	0.75	3.554	3.527	3.578	-0.008	-0.014
	1.00	3.000	2.952	–	-0.016	–
0.9	0.00	5.733	5.881	–	0.026	–
	0.25	5.156	5.276	–	0.023	–
	0.50	4.579	4.671	–	0.020	–
	0.75	4.053	4.066	–	0.003	–
	1.00	3.527	3.461	–	-0.018	–

Note: The normalized SIF K_{II}, established by the finite element method, is written in the form of correction function $Y_{FEM} = K_{II} \cdot t_0\sqrt{b} / P$, and for comparison of the results obtained in [16]. this function is given in the form $Y_{[16]} = f(\lambda, f_c) \cdot \sqrt{b} / \sqrt{H} / P$.

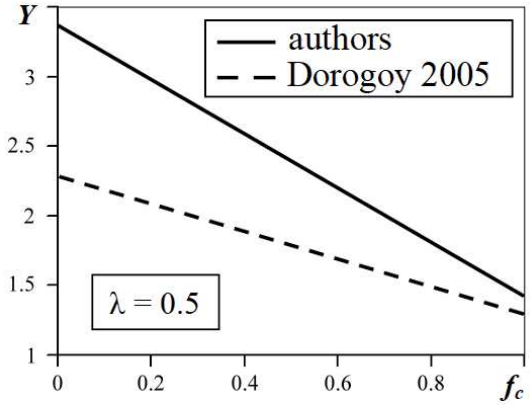

Fig. 10. Influence of the crack faces friction factor f_c on the normalized SIF K_{II} for different types of specimens

4. Conclusions

The new results of SIF K_{II} calculations for I-beam specimen are obtained by the finite element method. The corresponding K-calibration curves were built, by analyzing which it is established that the increase of crack faces friction factor by an order of magnitude monotonically reduces the normalized SIF K_{II} and this effect is almost 1.5 times greater for relative crack length 0.4 than for relative crack length 0.9.

The formula for SIF K_{II} calculation in the I-beam specimen considering crack faces friction factor is constructed. The results of calculations using this formula are compared with the results obtained by method of superposition of stressed states and finite differences method and their good convergence is shown.

The proposed calculation formula has an advantage before the known formula, because it can be used for SIF K_{II} calculation for the relative crack length range from 0.4 to 0.9 and crack faces friction factor range from 0 to 1. It is simple enough for application in engineering practice.

References

[1] K. Cvetkovski, J. Ahlstrom, M. Norell, C. Persson. Analysis of wear debris in rolling contact fatigue cracks of pearlitic railway wheels, Wear 314/1-2 (2014) 51-56, doi: https://doi.org/10.1016/j.wear.2013.11.049.

[2] O.P. Ostash, V.H. Anofriev, I.M. Andreiko, L.A. Muradyan, Kulyk V.V. On the concept of selection of steels for high-strength railroad wheels, Materials Science 48/6 (2013) 697-703, doi: https://doi.org/10.1007/s11003-013-9557-7.

[3] O.P. Datsyshyn. V.V. Panasyuk, Methods for the Evaluation of the Contact Durability of Elements of the Tribojoints (A Survey), Materials Science 52/4 (2017) 447-459, doi: https://doi.org/10.1007/s11003-017-9977-x.

[4] A.K. Hellier, K. Zarrabi, A.A. Merati, On the mode II fatigue threshold for mild steel, International Journal of Fracture 167/2 (2011) 267-272, doi: https://doi.org/10.1007/s10704-010-9540-3.

[5] M.O. Wang, R.H. Hu, C.F. Qian, J.C.M. Li, Fatigue crack growth under mode II loading, Fatigue & Fracture of Engineering Materials & Structures 18/12 (1995) 1443-1454, doi: https://doi.org/10.1111/j.1460-2695.1995.tb00867.x

[6] Y. Murakami, S. Hamada, A new method for measurement of mode II fatigue threshold stress intensity factor range $\Delta K_{\tau th}$, Fatigue & Fracture of Engineering Materials & Structures 20/6 (1997) 863-870, doi: https://doi.org/10.1111/j.1460-2695.1997.tb01530.x.

[7] C. Pinna, V. Doquet, The preferred fatigue crack propagation mode in M250 maraging steel loaded in shear, Fatigue & Fracture of Engineering Materials & Structures 22/3 (1999) 173-183, doi: https://doi.org/10.1046/j.1460-2695.1999.00161.x

[8] A. Otsuka, Y. Fujii, K. Maeda, A new testing method to obtain mode II fatigue crack growth characteristics of hard materials, Fatigue & Fracture of Engineering Materials & Structures 27/3 (2004) 203-212, doi: https://doi.org/10.1111/j.1460-2695.2004.00747.x.

[9] M. Liu, S. Hamada, Measurement of effective stress intensity factor range of mode II fatigue crack propagation, Procedia Engineering 10 (2011) 1949-1954, doi: https://doi.org/10.1016/j.proeng.2011.04.323.

[10] H. Matsunaga, N. Shomura, S. Muramato, M. Endo, Shear mode threshold for a small fatigue crack in a bearing steel, Fatigue & Fracture of Engineering Materials & Structures 34/1 (2011) 72-82, doi: https://doi.org/10.1111/j.1460-2695.2010.01495.x.

[11] V. Doquet, Q.H. Bui, G. Bertolino, E. Merhy, L. Alves, 3D shear-mode fatigue crack growth in maraging steel and Ti-6Al-4V, International Journal of Fracture 165/1 (2010) 61-76, doi: https://doi.org/10.1007/s10704-010-9504-7.

[12] G.V. Tsybanev, P.Y. Kravets, A.O. Khotsyanovskii, A method of testing for crack resistance under a cyclic shearing load, Strength of Materials 24/1 (1992) 97-103, doi: https://doi.org/10.1007/BF00777234.

[13] S. Okazaki, K. Wada, H. Matsunaga, M. Endo, The influence of static crack-opening stress on the threshold level for shear-mode fatigue crack growth in bearing steels, Engineering Fracture Mechanics 174 (2017) 127-138, doi: https://doi.org/10.1016/j.engfracmech.2016.12.007.

[14] H. Nishizawa, T. Ogawa, A mode II fatigue crack growth characteristics and experimental evaluation of the crack driving force, Journal of the Society of Materials Science 54/12 (2005) 1295-1300, doi: https://doi.org/10.2472/jsms.54.1295.

[15] T.M. Lenkovs'kyi, Determination of the characteristics of cyclic crack resistance of steels under transverse shear (a survey), Materials Science 50/3 (2014) 340-349, doi: https://doi.org/10.1007/s11003-014-9725-4.

[16] Ya.L. Ivanyts'kyi, T.M. Lenkovs'kyi, V.M. Boiko, S.T. Shtayura, Methods for the construction of the kinetic diagrams of fatigue fracture for steels under the conditions of transverse shear with regard for the friction of crack lips, Materials Science 49/6 (2014) 749-754, doi: https://doi.org/10.1007/s11003-014-9670-2.

[17] Y.L. Ivanytskyj, T.M. Lenkovskiy, Y.V. Molkov, V.V. Kulyk, Z.A. Duriagina, Influence of 65G steel microstructure on crack faces friction factor under mode II fatigue fracture, Archives of Materials Science and Engineering 82/2 (2016) 49-56, doi: https://doi.org/10.5604/01.3001.0009.7103.

[18] V.V. Kulyk, T.M. Lenkovs'kyi, O.P. Ostash, Mode I and Mode II Cyclic Crack Resistance of Wheel Steel, Strength of Materials 49/2 (2017) 256-262, doi: https://doi.org/10.1007/s11223-017-9865-5.

[19] T.M. Lenkovskiy, V.V. Kulyk, Z.A. Duriagina, R.A. Kovalchuk, V.G. Topilnytskyy, V.V. Vira, T.L. Tepla, O.V. Bilash, K.I. Lishchynska,

An effective crack tip region finite element submodel for fracture mechanics analysis, Archives of Materials Science and Engineering 87/2 (2017) 56-65, doi: https://doi.org/10.5604/01.3001.0010.7446.

[20] P.S. Kun, S.T. Shtayura, T.M. Lenkovs'kyi, Determination of the Stress Intensity Factor for a Transverse Shear Crack in a Beam Specimen, Materials Science 50/2 (2014) 212-216, doi: https://doi.org/10.1007/s11003-014-9710-y.

[21] A Dorogoy, L. Banks-Sills, Effect of crack face contact and friction on Brazilian disk specimens – A finite difference solution, Engineering Fracture Mechanics 72/18 (2005) 2758-2773, doi: https://doi.org/10.1016/j.engfracmech.2005.05.005.